Title: Isotopic insights into migration patterns of Pacific bluefin tuna in the eastern Pacific Ocean

Daniel J. Madigan[1]*[†], Zofia Baumann[1], Aaron B. Carlisle[2], Owyn Snodgrass[3], Heidi Dewar[4] & Nicholas S. Fisher[1]

[1]School of Marine and Atmospheric Sciences, Stony Brook University, Stony Brook, NY 11794, USA

[2]Hopkins Marine Station of Stanford University, 120 Ocean View Blvd, Pacific Grove, CA USA 93950

[3] Ocean Associates, Southwest Fisheries Science Center, NMFS, NOAA, La Jolla, CA 92037, USA

[4] Fisheries Resources Division, Southwest Fisheries Science Center, National Marine Fisheries Service (NMFS), National Oceanic and Atmospheric Administration (NOAA), La Jolla, CA 92037, USA

[†] Now at: Harvard University Center for the Environment, Harvard University, Cambridge, MA 02138, USA

*Harvard University, 26 Oxford Street, Cambridge, MA 02138

Tel (617) 496-7199; Fax (617) 496-7205

danieljmadigan@fas.harvard.edu

ABSTRACT

Understanding regional migration, residency dynamics, and associated trophic ecology can inform recovery strategies for pelagic species such as Pacific bluefin tuna *Thunnus orientalis* (PBFT). PBFT residency duration in the eastern Pacific is uncertain, particularly for larger individuals (here, >100 cm or ~3+ years of age). We applied a previously tested "chemical tracer toolbox (Fukushima-derived radiocesium and ^{13}C and ^{15}N stable isotope signatures) to examine migratory and residency patterns and dietary inputs of 428 age 1–6+ PBFT, collected from 2012 to 2015 in the eastern Pacific Ocean. Age 1–3 individuals were a mix of residents and recent (≤ 500 d) migrants, while 98% of age 3–4 and 100% of age 4–6.3 years old PBFT were resident for >500 days in the eastern Pacific. Zooplanktivorous forage (e.g., sardine, anchovy, pelagic red crab, and trophically similar species) of the California Current Ecosystem constituted 57–82% of diet across PBFT sizes. Migration timing estimates show that PBFT may spend two to five years in the eastern Pacific Ocean before returning to the western Pacific.

INTRODUCTION

Tuna species support global fisheries and are subjected to variable fishing pressures. Some species have been resilient to fisheries exploitation, while others have experienced marked population declines (Collette et al. 2011; Juan-Jordá et al. 2011). The bluefin tunas (Atlantic *Thunnus thynnus*, Pacific *T. orientalis*, and southern *T. maccoyii*) have experienced the most severe declines. Pacific bluefin tuna (PBFT) was recognized to be overfished in 2012 (ISC 2012), and the current estimated spawning stock biomass is 2–6% of unfished levels (ISC 2014, 2016). Insufficient understanding of the age/size structure, timing, and duration of migrations to and from the eastern Pacific Ocean limits informed, basin-wide recovery strategies for PBFT. A lack of information on temporal patterns of PBFT foraging ecology limits characterization of essential habitat, a critical component to ecosystem-based management (Pikitch et al. 2004). Here, we use two complementary migration tracers (radiocesium and stable isotope signatures) to assess trans-Pacific migration timing and eastern Pacific residency duration of PBFT captured in the eastern Pacific Ocean. We provide previously unavailable estimates of the migratory history of older PBFT (age classes 3–6), and use $\delta^{13}C$ and $\delta^{15}N$ values of PBFT and prey species to assess the general prey base that supports PBFT in the eastern Pacific Ocean.

The first large-scale studies of PBFT migration, using landings and conventional tagging data, showed that PBFT use both sides of the North Pacific Ocean as well as regions of the South Pacific Ocean (Bayliff et al. 1991; Bayliff 1994). The only known spawning grounds are in the western North Pacific Ocean, with spawning occurring in both the Sea of Japan to waters south of Japan and around the Nansei/Ryukyu Islands northeast of Taiwan to waters off the Philippines (Okiyama 1974; Kitagawa et al. 1995; Rooker et al. 2001). Conventional and electronic tagging studies revealed that some juvenile PBFT remain in waters around Japan in their first year

Bayliff 1994; Furukawa et al. 2016), while an unknown proportion of juvenile PBFT migrates to the eastern Pacific where they remain for several years before returning to the western Pacific (Bayliff et al. 1991; Bayliff 1993, 1994; Boustany et al. 2010). PBFT larger than 160 cm (≳5 years old) are caught primarily in the western North Pacific (Foreman & Ishizuka 1990), although some are caught in the South Pacific (Smith et al. 2001) and occasionally, with high temporal variability, in the eastern North Pacific (Foreman & Ishizuka 1990). Conventional tags provided the first insights into the migratory patterns and pathways of PBFT, but these studies included only smaller size classes, relied on fisheries for tag release and recapture, and provided no information on movements between tagging and recapture.

The development and use of electronic tags expanded understanding of tuna migrations, providing detailed information on movements over short and long timeframes (Kitagawa et al. 2000; Block et al. 2001; Fromentin & Powers 2005; Boustany et al. 2010; Block et al. 2011; Hartog et al. 2011; Furukawa et al. 2016). Electronic tagging of PBFT in the western Pacific provided some insight into eastward trans-Pacific migration (Kitagawa et al. 2009), although most western-tagged PBFT remained in the west Pacific, foraging around Japan and in the waters associated with the Kuroshio and Oyashio currents (Inagake et al. 2001; Kitagawa et al. 2002; Itoh et al. 2003b; Furukawa et al. 2016). In the eastern Pacific, electronic tags showed that PBFT largely remained within the eastern Pacific for a number of years, migrating in a seasonal north-south pattern (Domeier et al. 2005; Boustany et al. 2010). These data demonstrated that once in the eastern Pacific, age 1–4 PBFT show a high degree of residency in the region before returning to the western Pacific (Boustany et al. 2010).

While conventional and electronic tags have provided important information on PBFT movements and habitat use, they have provided only limited information on the dynamics of

migration to the eastern Pacific. This is due to few recoveries of western-tagged PBFT in the east, and thus far only one electronically tagged individual has made the eastward trans-Pacific migration (Itoh et al. 2003a; Kitagawa et al. 2009). PBFT tagged in the eastern Pacific provide no insight into migratory history prior to tagging. As a result, there are data gaps in our understanding of west-east movements, how these movements relate to size structure and catch in the eastern Pacific, and the environmental forcing mechanisms associated with trans-Pacific migration. Since PBFT are subject to different size-dependent fishing pressures in the eastern versus western Pacific Ocean, the amount of time spent in the eastern Pacific will affect fisheries mortality for juvenile PBFT (Aires-da-Silva et al. 2009).

In recent years, a number of chemical tracers have been developed that allow scientists to assess the migratory history of captured individuals. This approach can be viewed as a tag-recapture study with 100% recapture rate over the life of the tracer, as every fisheries-captured individual provides 'tag location' (inferred region of origin), recapture location, and in some cases, estimated time-at-large (using turnover rates of the intrinsic chemical tracer). Isotopic clock techniques (Phillips & Eldridge 2006; Buchheister & Latour 2010; Klaassen et al. 2010) allow estimates of time-of-entry into a new marine ecoregion. For PBFT, complementary chemical tracers in the form of radiocesium isotopes (^{134}Cs and ^{137}Cs, or ^{134,137}Cs) released in 2011 from the damaged nuclear power plant in Fukushima, Japan, have been combined with stable isotope ratios of carbon and nitrogen (δ^{13}C and δ^{15}N) (Madigan et al. 2014). Similar information has been obtained from otolith microchemistry, albeit for a limited number (n = 25) of PBFT thus far (Baumann et al. 2015). The complementary radionuclide and stable isotope tracers were used to understand migration patterns and to differentiate migrant and resident PBFT in the eastern Pacific (Madigan et al. 2012a, 2013, 2014), though these studies were

largely limited to 1–3 year old PBFT. A recent study also used $\delta^{15}N$ values of PBFT in the western Pacific to identify eastern Pacific migrants that had recently returned to the Sea of Japan (Tawa et al. 2017).

In addition to its use as a migration tracer, stable isotope analysis (SIA) has been used to assess trophic dynamics in aquatic systems (Post et al. 2000; Clementz & Koch 2001; Davenport 2002; Revill et al. 2009; Graham et al. 2010; Carlisle et al. 2012; Madigan et al. 2012b). Ecological drivers (e.g., prey availability) have been suggested for both PBFT emigration from the western Pacific (Polovina 1996) and retention within the highly productive eastern Pacific (Boustany et al. 2010). The ability to identify migratory history increases the value of SIA as a tool for inferring trophic patterns. Separating PBFT migrants from residents, coupled with quantified stable isotope turnover and diet-tissue discrimination factors in PBFT (Madigan et al. 2012c; Bradley et al. 2014), allows for analytical tools such as Bayesian stable isotope mixing models (Phillips & Gregg 2003; Moore & Semmens 2008) to be used to describe the foraging ecology of PBFT while resident in the eastern Pacific.

Past studies using chemical tracers in PBFT (Madigan et al. 2012a, 2013, 2014) provided new information on PBFT migration dynamics in the eastern Pacific, but were limited to age 1–3 PBFT. Here we use chemical tracers to describe migration timing and trophic dynamics of 428 PBFT migrating to the eastern Pacific, spanning sizes 61−192 cm (age classes 1 to 6) for more robust estimates of west-to-east migration and ecology across PBFT age. Results advance efforts to understand the ecological drivers underlying PBFT movement to and residency in the eastern Pacific Ocean.

MATERIALS & METHODS

Ethics Statement

All research and associated tissue sampling was carried out under the State of California Department of Fish and Wildlife permit #SC-12372 issued to the National Oceanic and Atmospheric Administration Southwest Fisheries Science Center (NOAA SWFSC).

Sampling and Analysis of PBFT and Prey Tissues

PBFT were caught in waters off central and southern California, USA and northern Baja California, Mexico between 2012 and 2015. All available size classes were sampled for muscle tissue, and largest and smallest PBFT were targeted when available to maximize the represented size range. Fish were sampled in all months that they were available. Samples were primarily obtained from fish captured by recreational anglers and landed in San Diego, CA, as part of an ongoing effort by NOAA SWFSC. PBFT were also caught by experimental deep set long-line during research cruises conducted by NOAA aboard F/V Ventura II. Approximately 20 g of white muscle tissue was collected for SIA, and when possible, 300 g for gamma-analysis of ^{134,137}Cs. Length (fork length or FL: length from tip of snout to fork of tail, cm) was measured directly or calculated from operculum length (length from tip of snout to posterior edge of gill plate) following the regression in Madigan et al. (2013). Measured or calculated FL, date, and capture location were recorded for all individuals. Length (cm) was used to estimate age in years using the fixed growth curve reported in Shimose et al. (2009). All ages reported hereafter are calculated from length, and are therefore size-based estimates of PBFT age.

White muscle tissue was immediately stored and frozen at -5°C. Samples were then frozen at -80°C for 24h, lyophilized for 72h, and homogenized using a Wig-L-Bug (Sigma

Aldrich). Activity levels of Fukushima-derived radionuclides (^{134,137}Cs) were measured in all PBFT for which sample tissue was sufficient for analyses in 2012 and 2013. ^{134,137}Cs activity (Bq kg^{-1} dry mass) was analyzed using broad-energy germanium detectors (Canberra). ^{134,137}Cs activities were decay-corrected to angler-estimated catch date for each fish. Lower limits of detection were sample dependent and ranged from <0.01 to 1.0 Bq kg^{-1} dry wt for both ^{134}Cs and ^{137}Cs. See Madigan et al. (2012a, 2013, 2014) for full description of sample preparation and gamma-analysis methodology.

Collection of appropriate prey items was informed by published descriptions of PBFT diet in the eastern Pacific (Pinkas 1971; Madigan et al. 2012b, 2015; Shimose & Wells 2015) (see Table S1 for sampled prey species). Pelagic prey species including fish, cephalopods, and crustaceans were collected whole, either from NOAA sampling cruises or sampled from stomach contents of tunas (*T. orientalis*, *T. albacares*, and *T. alalunga*) and opah (*Lampris guttatus*) collected in the eastern Pacific. Only intact, recently consumed prey were sampled for muscle tissue (5-20 g). For prey fish, white muscle was sampled from the dorsal musculature. For squids, a section of mantle tissue was collected. Small crustaceans (krill and amphipods) were analyzed whole; larger pelagic red crab *Pleuroncodes planipes* were subsampled for tail white muscle tissue as described in Madigan et al (2012b).

Analyses of δ^{13}C and δ^{15}N were performed at the University of Hawaii using an on-line C-N analyzer coupled with a Delta XP isotope ratio mass spectrometer. Replicate reference materials of atmospheric nitrogen and V-PDB were analyzed every 10 samples, and analytical precision was <0.2‰ for δ^{13}C and δ^{15}N. δ^{13}C values of PBFT and prey were arithmetically lipid-normalized based on mass C:N ratios using taxon- or species-specific lipid normalization algorithms (Logan et al. 2008). δ^{13}C and δ^{15}N values are reported in parts per mille (‰).

175

176 **Migration classification and timing estimates**

177 Presence of ^{134}Cs in PBFT muscle was demonstrated previously as an unequivocal tracer
178 of migration from the western to eastern Pacific (Madigan et al. 2013, 2014). Accordingly, all
179 fish with detectable activity of ^{134}Cs were categorized as recent migrants (within ~ 1.5 yr) from
180 the western Pacific. Since lack of ^{134}Cs cannot definitively rule out recent migration, we used
181 SIA to secondarily characterize all PBFT. PBFT analyzed for both ^{134}Cs and SIA were used to
182 determine the $\delta^{15}N$ values of migrants, and all PBFT were secondarily categorized based on their
183 $\delta^{15}N$ values. Following Madigan et al. (2014), $\delta^{15}N$ values from PBFT containing ^{134}Cs (known
184 migrants) and $\delta^{15}N$ values of yellowfin tuna (known to be eastern residents; Madigan et al.
185 2012b) were used as training data. This approach requires $\delta^{15}N$ values of yellowfin and PBFT at
186 isotopic steady-state in the eastern Pacific to be similar, which was demonstrated in Madigan et
187 al. (2014). Discriminant analysis assigned a classification (migrant or resident) for each PBFT
188 and reported a classification error value indicating the proportion of individuals with inconsistent
189 classification assignments (Klecka 1980). The timeframe of a 'recent' migrant, used throughout,
190 refers to ~500 days which represents three muscle $\delta^{15}N$ half-lives in captive PBFT (Madigan et
191 al. 2012c) as applied in previous studies (Madigan et al. 2014, 2015). This timeframe (~500
192 days) likely varies with PBFT size, as positive allometric scaling of turnover rate has been shown
193 in fish (Weidel et al. 2011). While allometric scaling of turnover rate with size will influence
194 estimated length of time since migration, it will not affect categorization of migrants and
195 residents. We used the same timeframe across sizes due to the narrow size range of observed
196 migrants (see Results) and the lack of a quantitative allometric relationship specific to large

pelagic fish. PBFT age was estimated and individuals grouped into discrete age classes based on length-at-age relationships reported in Shimose et al. (2009).

Bootstrap analysis was used to generate a distribution of estimated residency times (time between PBFT entry to eastern Pacific waters and time of capture/sampling) for each individual PBFT. For bootstrap analysis, we used an isotopic clock for $\delta^{15}N$ based on Klaassen et al. (2010). This method has been applied previously to PBFT in the eastern Pacific (Madigan et al. 2014), and assumes similar end-member values across small PBFT in the western and eastern Pacific as well as isotopic turnover parameters. The bootstrapping approach (in contrast to single estimates for each PBFT) allowed the analysis here to account for variability in end-member values and turnover rate of $\delta^{15}N$. Assumptions based on smaller PBFT were deemed appropriate here as isotopic clock calculations were applied only to migrants, and all but one migrant were <3 yr (see Results). PBFT $\delta^{15}N$ values, estimated end-member values for the eastern and western Pacific, and turnover parameters for ^{15}N in PBFT were used in isotopic clock estimates (see below). As isotopic clock techniques can only be used during transition between diets, and cannot be used once consumers have reached steady-state with the new diet, the isotopic clock was used to estimate the period of residency only for migrant PBFT. Since isotopic clock approaches estimate time since shift to feeding in sampling region, these estimates reflect time since entry in the eastern Pacific Ocean and not estimated time of departure from the western Pacific Ocean.

Isotopic clock estimates use the following equation from Klaassen et al. (2010)

$$t_i = \frac{\ln\left(\frac{\delta_{0_i} - \delta_{f_i}}{\delta_t - \delta_{f_i}}\right)}{\lambda_i} \quad (1)$$

where t = time (days) in the eastern Pacific, i = number of iterations, λ is the first-order rate constant for turnover of ^{15}N in PBFT muscle, and δ_0, δ_f, and δ_t represent the initial $\delta^{15}N$ end-member from the western Pacific, the final $\delta^{15}N$ end-member from the eastern Pacific, and the measured $\delta^{15}N$ at time t, respectively. For isotopic clock calculations, we used the tissue turnover rate for PBFT ($\lambda = 0.00415 \pm 0.001$) from Madigan et al. (2012). We used $\delta^{15}N$ values representative of PBFT in equilibrium with western Pacific prey (11.0 ± 1.1 ‰), assuming similar feeding across small PBFT (Madigan et al. 2014) as the initial $\delta^{15}N$ value endmember (δ_0). The $\delta^{15}N$ value from 109 yellowfin tuna residential to the eastern Pacific (15.4 ± 0.8 ‰; Madigan et al. 2014) was used as the final endmember (δ_f) in the isotopic clock model (Klaassen et al. 2010). Due to the uncertainty around estimating PBFT age from size (Shimose et al. 2009), we also bootstrapped age estimates using measured PBFT length and the length-age algorithm and associated error values reported in Shimose et al. (2009). For each PBFT, isotopic clock estimates of the period of residency were bootstrapped (1000×) by randomly sampling from mean (±SD) starting endmember and the mean (± SD) $\delta^{15}N$ turnover rate of muscle. Bootstrapped isotopic clock estimates of residency time were used to estimate age at arrival by subtracting clock estimate from bootstrapped size-estimated age at capture for all migrant fish. Since resident PBFT are at steady-state with isotopic conditions of the eastern Pacific, isotopic clock techniques could not be applied. Therefore, we estimated residency time of resident PBFT by resampling the distribution of estimated age of migrant arrival (1000×) and subtracting those values from estimated age at capture for each resident. This approach assumes the distribution of age at arrival of migrants to be representative of the likely migratory history of residents. We then fit a linear regression (based on maximizing adjusted R^2 compared to other fits) to the

241 relationship between age at capture and estimated residency time in the eastern Pacific. Analyses
242 were performed using Matlab R2013b.
243
244 **Trophic analyses**
245 The relative proportion of four prey groups (pelagic macrozooplankton, pelagic forage
246 prey, larger pelagic prey, and coastal prey) in PBFT diet was assessed using the Bayesian mixing
247 model MixSir (Moore & Semmens 2008). These prey groupings were based on both common
248 trophic level (based on similar of $\delta^{13}C$ and $\delta^{15}N$ values) using cluster analysis (Madigan et al.
249 2012b) and location of collection (inshore versus offshore/pelagic). Clustering prey values
250 maximized prey group differentiation in $\delta^{13}C$ versus $\delta^{15}N$ graphical space, which allowed for
251 more constrained mixing model estimates. Coastal prey, which were higher in both $\delta^{13}C$ and
252 $\delta^{15}N$ than pelagic analogs, were included to investigate potential shifts in foraging habitat to
253 inshore foraging regions or inshore prey being encountered offshore by resident PBFT. Groups
254 included the following species: pelagic macrozooplankton (euphausiids and amphipods), pelagic
255 forage prey (zooplanktivorous small fish, squids, and pelagic red crab), larger prey (mackerels,
256 jumbo squid, and bonito), and coastal prey (nearshore-collected sardine, pacific mackerel, jack
257 mackerel, topsmelt, and large market squid) (See Table S1 for species and isotopic values). For
258 mixing model runs, we used diet-tissue discrimination factors (DTDFs) from Madigan et al.
259 (2012c) which are specific to PBFT. Inputs were $\delta^{13}C$ and $\delta^{15}N$ values of resident PBFT
260 (grouped by age class) and the calculated mean (± SD) $\delta^{13}C$ and $\delta^{15}N$ values of the four prey
261 groups. We generated median and 95% credible intervals for the proportion of each prey group
262 in diet of each PBFT age class. We ran 10^6 iterations and uninformed priors (no *a priori*
263 proportional diet estimates) when generating mixing model results.

Individual PBFT categorized as eastern Pacific residents were grouped by age and compared to assess potential differences in $\delta^{13}C$ and $\delta^{15}N$ due to size-based foraging differences in the eastern Pacific. We compared $\delta^{13}C$ and $\delta^{15}N$ across age classes using the non-parametric Mann Whitney U-test. Linear regression was used to test for significant changes in $\delta^{15}N$ and $\delta^{13}C$ across PBFT size (to assess ontogenetic trends) and across months of sampling (to assess potential seasonality of prey $\delta^{13}C$ and $\delta^{15}N$ values in the eastern Pacific). Statistical analyses were performed using Matlab vR2015a.

RESULTS

We obtained samples for SIA from 428 PBFT, of which 272 were also sampled for radiocesium analysis. Sampled PBFT ranged in size from 61 to 191.5 cm FL (size-estimated age: 1.2 to 6.3 years old) (Shimose et al. 2009). Sample sizes for SIA were age class 1-2 (n = 180), age class 2-3 (n = 162), age class 3-4 (n = 46), age class 4-5 (n = 20), and age classes 5-7 (n = 20).

The only radionuclide that unequivocally represents exposure to Fukushima-contaminated waters and/or prey (^{134}Cs) was not detectable in 2014 and 2015 samples. In 2013, ^{134}Cs was detected in most (81%) but not all known migrants from the western Pacific, demonstrating that the use of ^{134}Cs as an unequivocal tracer had diminished by 2013 and expired by 2014. In 2012 and 2013 PBFT, ^{134}Cs was detected in 107 (39%) samples (n = 93 in 2012, n = 14 in 2013; Figure 1). Mean ^{134}Cs activity in these PBFT was 0.7 ± 0.4 Bq kg^{-1} (excluding one aberrantly high activity level of 7.4 Bq kg^{-1}). These 95 fish also showed ^{137}Cs activities higher (2.1 ± 0.9) than pre-2011 'background' values (~1–1.5 Bq kg^{-1}) and ^{134}Cs:^{137}Cs ratios of 0.09 to

0.46 (0.31 ± 0.08) (Figure 1). The individual PBFT with highest ^{134}Cs (7.4 Bq kg^{-1}) also had the highest ^{137}Cs (13.1 ± 0.9 Bq kg-1) and a slightly higher ^{134}Cs:^{137}Cs ratio of 0.57 ±0.05. PBFT defined as residents by discriminant analysis of δ^{15}N values (n = 182) showed lower ^{137}Cs activities (1.1 ± 0.4 Bq kg^{-1}) than migrants (2.1 ± 0.9 Bq kg^{-1}). All PBFT with detectable levels of ^{134}Cs were <3 years old and <100 cm (Figure 1). An exponential decline in ^{134}Cs activities was observed in PBFT from August 2011 (reported in Madigan et al. 2012a) to the end of 2013, due to the half-life of ^{134}Cs (2.1 years), dispersal and dilution in the western Pacific, and metabolic elimination. This allowed for the calculation of effective half-life of ^{134}Cs in PBFT exposed to Fukushima radiocesium, which was estimated to be 151 days following first catch of ^{134}Cs-contaminated PBFT in 2011 (Figure 2).

Stable isotope values of δ^{15}N and δ^{13}C were measured in 428 PBFT. Discriminant analysis categorized these 428 PBFT as migrants or residents with a classification error of 2.2%. δ^{15}N values of migrants (11.3–14.6 ‰) and residents (14.7–17.4 ‰) were similar to those reported previously for PBFT in the eastern Pacific, and classification error occurred only in PBFT with intermediate values (14.5-14.8 ‰). δ^{15}N values increased with size in migrants, while residents reached apparent steady-state (Figure 3). δ^{13}C was more variable in migrants than in residents >3 years old, with some migrants showing either higher and lower values than residents (Figure 3). When both Cs and SIA were analyzed in the same fish, δ^{15}N- and ^{134}Cs-defined migratory status agreed 100% (Figure 3). There was no evidence for false positives (detecting ^{134}Cs in PBFT residents) but some δ^{15}N-categorized migrants showed no ^{134}Cs, and were thus false negatives (i.e., they were recent migrants based on δ^{15}N, but did not show detectable ^{134}Cs activity) for ^{134}Cs (Figure 3). All false negatives were for PBFT collected in 2013. Based on δ^{15}N

values, 106 of 107 migrants were in age classes 1-3 (length 60 to 96.5 cm), with one PBFT of 123.3 cm (~3.6 years old) with a $\delta^{15}N$ value (13.4 ‰) consistent with migrants (Figure 3).

The proportion of residents increased by age class: 1-2: 20% (36 of 180), 2-3: 67% (109 of 162), 3-4: 98% (45 of 46), 4-5: 100% (20 of 20), and 5-7: 100% (20 of 20; age class 5-6 and 6-7 combined due to low n of age class 6-7) (Figure 4). All PBFT < 70.7 cm were recent migrants, with residents in age class 1-2 significantly larger (70.7 – 79.8 cm; 76.3 ± 2.5 cm) than migrants (61 – 79.8 cm; 69.1 ± 3.6 cm). All age class 1-2 PBFT categorized as residents were the larger PBFT in this group (1.6 to 2.0 years old; see Figure S1). After age two, residency period in the eastern Pacific Ocean generally increased linearly with PBFT age, with the oldest PBFT (age classes 3-7) spending from two to more than five years in the eastern Pacific (Figure 4). Isotopic clock estimates indicated most PBFT migrated to the eastern Pacific Ocean between age ~0.5 and ~1.3 yrs (1.0 ± 0.3 yrs), with a second smaller pulse at ages 1.2 to 2 yrs (1.3 ± 0.5 yrs) (Figure 5). Peak arrival time estimates were from April to June across years of sampling, with time-of-arrival curves showing a left-skewed distribution with a single peak (Figure 6). A linear fit best described the relationship between age at capture and estimated residency time in the eastern Pacific (adjusted $R^2 = 0.85$; Figure 4).

Grouping of PBFT into residents and migrants allowed for stable isotope-based analyses of diet for PBFT residents only (n = 230). $\delta^{13}C$ and $\delta^{15}N$ values of 217 individual prey items representing 18 species were included in diet analyses (Table S1). Prey groupings were discrete in $\delta^{13}C$ versus $\delta^{15}N$ isospace, with minimal overlap between prey groups (Figure 7). $\delta^{13}C$ and $\delta^{15}N$ of PBFT age groups, once corrected for DTDF of PBFT, mostly overlapped with pelagic forage base of the eastern Pacific which includes zooplanktivorous small fish, small squids, and pelagic red crab. Mixing model results showed that all resident PBFT relied heavily on the

pelagic forage base (57-82%; mean across age classes 73 ± 10%) (Figure 7), though smallest PBFT had most mixed diet with more inputs of pelagic macrozooplankton (Figure 7). Although mixing model results were similar across PBFT age (high use of pelagic forage base, some use of pelagic macrozooplankton, minimal use of larger pelagic prey or inshore prey; Figure 7), pairwise age comparisons of $\delta^{15}N$ and $\delta^{13}C$ showed significant differences between some age classes, particularly age 1-2 which had significantly lower $\delta^{15}N$ values than older age classes (Table S2).

DISCUSSION

A combination of naturally-occurring and anthropogenic chemical tracers provided information on the migratory history, arrival times, and foraging ecology of PBFT in the eastern Pacific Ocean. Insights gained here are particularly useful for larger PBFT, for which information on migratory history and ecology has been limited. Collectively, our data suggest that PBFT typically arrive in the eastern Pacific before age 2, PBFT >3 years old have been residential to the eastern Pacific for at least ~500 days, and the highly abundant zooplanktivorous forage base of the eastern Pacific (e.g., forage fish, squids, pelagic red crabs) supports PBFT in this region. Consequently, the presence of large PBFT (e.g., >100cm) in the eastern Pacific fishery relies upon multi-year residence and survival of smaller size classes, and residence is likely correlated with favorable foraging conditions.

Combining radiocesium and SIA allowed for evaluation of the applicability of the radiocesium tracer over time. Radiocesium levels in the smallest PBFT (<70 cm) were used to gauge the reliability of this tracer, as these fish are known to be recent migrants from the western

Pacific (Bayliff et al. 1991; Bayliff 1994). Activities of ^{134}Cs decreased in these small PBFT from 2011 to 2013 (Figure 2), which was expected based on dispersal, dilution, and decay of Fukushima radiocesium (Buesseler et al. 2011; Nakano & Povinec 2012; Madigan et al. 2013, 2014). All small (<70 cm) PBFT had measurable ^{134}Cs in 2012 (Madigan et al. 2013), but by 2013 ^{134}Cs was undetectable in 19% of known migrants, showing that ^{134}Cs was no longer a completely reliable tracer of migration from the west Pacific Ocean. The calculated biological half-life of ^{134}Cs in PBFT of 151 days (Figure 2) combines biological turnover and radioactive decay. Human health risk from levels reported in 2011 PBFT was extremely low (Fisher et al. 2013), and data here show near-zero levels of Fukushima-derived ^{134}Cs in PBFT captured in 2013-2015. This confirms the assertion that Fukushima-derived radiocesium was a transient tracer (Madigan et al. 2012a, 2013). While ^{137}Cs, released from Fukushima in a 1:1 ratio to ^{134}Cs, has a longer half-life ($t_{1/2}$ = 30 yr) and was at higher activities in migrants, existence of pre-2011 ^{137}Cs (from weapons testing, and currently at low levels) and variability in that background complicate use of ^{137}Cs as an unequivocal migration tracer. However, ^{134,137}Cs was a useful tracer from 2011–2013 PBFT that subsequently ground-truthed the natural tracers δ^{15}N and δ^{13}C.

Results demonstrated the utility of using SIA to understand animal migrations. δ^{15}N values functioned as a diagnostic tracer of trans-Pacific migration, while δ^{13}C did not (Figure 3). Recent migrants showed lower δ^{15}N characteristic of the western Pacific (Madigan et al. 2014), with some intermediate δ^{15}N values due to partial equilibration to higher δ^{15}N characteristic of the eastern Pacific pelagic food web. For PBFT > 100 cm, 98% showed high δ^{15}N (14.7 – 17.4‰) indicating they were at steady-state with eastern Pacific prey (Madigan et al. 2012b, 2014) (Figure 3). δ^{13}C values in migrants (-16.1 to -19.4‰) were more variable than in residents (-16.1 to -18.4‰), which also appeared to reach steady-state with δ^{13}C in the eastern Pacific at

sizes ≥ ~100 cm (Figure 3). The source of $\delta^{13}C$ variability in migrants is unclear, as migrants showed values both higher (> -17.5‰) and lower (< -19‰) than residents (Figure 3). It is possible that different regional origins in the western Pacific Ocean produce these variations. It has been suggested that juveniles migrate to the eastern Pacific from either the East China Sea or South Japan waters (Fujioka et al. 2015), and these regions have higher and lower $\delta^{13}C$ prey (Madigan et al. 2016), respectively, than prey in the eastern Pacific Ocean (Madigan et al. 2012b). Both the utility of $\delta^{13}C$ as a more specific tracer of western Pacific origin and potential migratory differences between regional groups could be assessed in future studies directly measuring $\delta^{13}C$ in western Pacific PBFT. Combining $\delta^{13}C$ and $\delta^{15}N$ data in future studies could inform emigration rates of PBFT into the eastern Pacific Ocean from different PBFT spawning grounds, including potential mixing over time, and may be applicable to other migratory species (e.g. albacore *Thunnus alalunga*; Wells et al. 2015) in the North Pacific Ocean.

Results from this study confirm that bluefin tuna migrating to the eastern Pacific arrive in two pulses, either in their first or second year, with minimal new arrivals in subsequent years of life. This mirrors conclusions from previous conventional tag-recapture studies (Bayliff et al. 1991; Bayliff 1994) conducted several decades prior, demonstrating the continuity of juvenile PBFT migration patterns and corroborating the tracer-based approach. It should be noted that while reporting age estimates is important for framing migration in the context of PBFT ontogeny, length-at-age estimates for PBFT show substantial variability (see Shimose et al. 2009). Age estimates are provided here for a temporal picture of PBFT movements, but in this study reported lengths provide the most accurate information as a directly measured proxy for PBFT lifestage.

All age 1-2 residents were in the latter half of their second year of age (1.6–2.0 years old; Figure 5); isotopic clock estimates suggest these fish migrated to the eastern Pacific Ocean between age ~0.5 and ~1.2 yrs (1.0 ± 0.3 yrs), with a second smaller pulse at ages 1.2 to 2 yrs (1.3 ± 0.5 yrs) (Figure 5). The earlier estimated ages of arrival (i.e. 0.5 to 1 year) are in contrast to observed movements of age-0 PBFT off Japan (Furukawa et al. 2016) and a lack of age-0 fish in eastern Pacific catch data (Bayliff 1994). However, previous analyses of PBFT otoliths demonstrate entry of age-0 PBFT in the eastern Pacific. Baumann et al. (2015) used otolith microstructure analysis to estimate age (days) and otolith trace element composition to estimate eastern Pacific arrival times of juvenile PBFT caught off Southern California. Of 24 PBFT analyzed, 4 were less than 1 year old (328 to 361 days) at time of capture in the eastern Pacific, and trace element analyses suggested age-of-entry as low as ~0.7 years (Baumann et al. 2015). Since PBFT are born in summer (Okiyama 1974; Tanaka et al. 2007), these youngest migrants would arrive in the east in winter/spring, and eastern catch would likely not include these migrants until summer (when they are ~1 year old) due to the seasonality of fishing effort in the east (generally May to October; Baumann et al. 2015). However, some of these lower (and higher) estimates of age-at-arrival may also be an artefact of isotopic clock estimates. As isoclock calculations account for uncertainty of end-members and turnover rates, combinations of outlier values will result in unrealistic ‘tails’ in distributions (Klaassen et al. 2010; see Figures 5 and 6). Due to such artefacts, overall patterns of isoclock estimates (e.g. peaks of timing estimates) should be considered more robust than tail values in estimate distributions.

The two peaks in arrival time by age do not appear to correspond with two peak seasonal arrival times in the eastern Pacific, as arrival times across years appear to be an extended pulse from winter to summer that centers around April (Figure 6). Peak arrival in the eastern Pacific in

April is similar to previous isotope-based estimates (Madigan et al. 2014), later than a single electronically tagged PBFT that arrived in the eastern Pacific from Japan in January (Kitagawa et al. 2009), slightly earlier than tag-recapture and catch-based estimates of May to October (Bayliff et al. 1991), and earlier than otolith microchemistry-based estimates of June to August (Baumann et al. 2015). The isotope approach used here circumvents the spatial and temporal patterns that influence conventional tag-recapture and catch-based estimates, and isotopic results show that PBFT captured in June to August have actually been in the eastern Pacific for several months (Figure S4). Inaccuracies of isotopic-based arrival time estimates here could partially be caused by varying rates of ^{15}N turnover, which can change with individual growth rates (Madigan et al. 2012c) and animal size (Weidel et al. 2011). Otolith microchemistry and microstructure analysis is a promising approach as it identifies not only time-of-entry into water masses of distinctive geochemical properties, but also more accurate PBFT age-at-entry (Baumann et al. 2015). Baumann et al. (2015) found that length-based age was overestimated compared to age determined by microstructure analysis. This approach has yet to be performed on large sample sizes of PBFT, but could provide more accurate times and ages of entry of PBFT to the eastern Pacific. Increased archival tagging efforts in the western Pacific would provide precise estimates of migration timing, as recoveries thus far (Kitagawa et al. 2009) have been insufficient to determine patterns of west-east movements. Complementary analyses, particularly when applied to the same individual PBFT, inform isotope-based inferences, which can be applied to large sample sizes for relatively efficient and economical population-wide estimates of movements.

Over four years of study, there was apparent inter-annual variability in migration timing. Peak estimated arrival times in 2014-2015 were slightly earlier and broader than in 2012-2013

(Feb–May vs April–May; Figure 6). This broader arrival window may be linked to increased sea surface temperatures and/or oceanographic conditions associated with ENSO or 'The Blob', which ostensibly altered migration patterns of migratory marine species (Kintisch 2015). ENSO-associated changes likely impacted abundance and/or distribution of prey in the western Pacific, which has been linked with the rate of eastward PBFT migration (Polovina 1996). Sustained warm ocean temperatures potentially broadened the temporal window of optimal water temperatures for PBFT migrations, which have been tightly linked with ocean temperature (Kitagawa et al. 2007; Boustany et al. 2010) potentially due to PBFT physiological constraints (Whitlock et al. 2015). Thus warmer years in the eastern Pacific may expand the range of PBFT arrival times. Higher water temperatures also coincided with higher catch rates of PBFT in winter months, and we were able to assess migration patterns of these small PBFT. Isotopic ratios showed that these fish were not immigrating from the western Pacific in winter months but rather had been resident in the eastern Pacific for several months (Figure S4). This indicates that observed PBFT presence at higher latitudes in winter months was not due to altered trans-Pacific migration timing, but rather a change in the typical timing or latitudinal distribution of PBFT in the eastern Pacific. PBFT generally migrate to warmer southern waters in winter, presumably for thermal refuge (Domeier et al. 2005; Boustany et al. 2010; Whitlock et al. 2015). Abnormally warm water masses in winter of 2014 and 2015 as far north as the Southern California Bight shifted optimally warm waters (16°-18°C; Whitlock et al. 2015) substantially northward, potentially retaining PBFT in the region.

Results here advance understanding of larger size classes of PBFT in the eastern Pacific due to availability of larger PBFT in 2014 and 2015. PBFT age >3 were predominantly resident (98.8%) to the eastern Pacific (Figures 3 and 4). Spawning PBFT in the Sea of Japan, which are

smaller than PBFT in the southern spawning grounds, have been reported as 50% and 95% mature at 114.4 cm (~3.2 years) and 133.6 cm (4 years), respectively (Shimose et al. 2009; Okochi et al. 2016). Accordingly, all PBFT older than 3.2 years in this study were of ages at which spawning is possible. However, there is no evidence of spawning in the eastern Pacific based on larval tows (Nishikawa 1985), and a small number of large (160-180 cm) female PBFT showed no gonadal evidence of recent spawning based on histology (authors unpubl. data). Thus the eastern Pacific Ocean can harbor PBFT for several years past the reported size at first sexual maturity. If the larger sized PBFT analyzed here spawn in their first year of return to the western Pacific, it is most likely these PBFT use the Sea of Japan spawning grounds based on the smaller size and lower age PBFT observed there (Chen et al. 2006; Okochi et al. 2016). Recent isotopic analyses of PBFT from the Sea of Japan indeed revealed substantial proportions of eastern migrants in age 4 (20%), age 5 (19%), age 6 (33%), and age 7-17 (67%) PBFT, though more samples need to be analyzed over time to obtain population-wide estimates and temporal variability (Tawa et al. 2017).

A more comprehensive, quantitative assessment of trans-Pacific movement dynamics would ideally be achieved by a coordinated stable isotope study, using accretionary structures (otoliths) and dynamic tissue (muscle), on both sides of the Pacific Ocean. Ongoing sampling of PBFT 2 to 7 years old in the western Pacific will clarify departure rates from the eastern Pacific across age classes, time lags between departure from the east and spawning in the west, and contribution of eastern migrants to spawning stock biomass (Tawa et al. 2017) with the limitation that the muscle isotope signal degrades after ~500 days (Madigan et al. 2012c). For older PBFT (~7 to 26 years old) captured in the southern spawning ground northeast of Taiwan, < 2% had bulk and amino acid isotope values consistent with the eastern Pacific (Madigan et al.

492 2016). Overall frequency and age distribution of trans-Pacific migration can be comprehensively
493 described only with a bilateral study. Combining isotopic analyses and electronic tagging would
494 generate both retrospective and prospective migration data from simultaneously sampled and
495 tagged PBFT.

496 Measurements of ^{134}Cs provided additional insight into the geographic origin of trans-
497 Pacific migrants. Detection of ^{134}Cs in 2012 (Madigan et al. 2013) contrasts with measurements
498 in PBFT caught in Japan, where many PBFT sampled in 2012 were below detection limits
499 (MAFF 2015). In seawater, high levels of Fukushima-derived radiocesium were confined to a
500 relatively small ocean region off eastern Japan, north of the Kuroshio Current (Buesseler et al.
501 2012; Rypina et al. 2013). This region was utilized for several months by an electronically-
502 tagged PBFT that subsequently migrated to the eastern Pacific (Kitagawa et al. 2009) (Figure 8).
503 Juvenile PBFT in the western Pacific also use other regions in the Sea of Japan and south of
504 Japan (Fujioka et al. 2015), where exposure to Fukushima radiocesium would be minimal. The
505 high incidence of radiocesium detection in 2011 and 2012 eastern Pacific PBFT suggests that
506 this region off eastern Japan is a staging ground for eastward trans-Pacific migration (Figure 8).
507 If this is the case, regional differences in the magnitude of commercial fishing effort on ages 0-2
508 year PBFT around Japan could influence the biomass of PBFT migrating to the eastern Pacific,
509 and future tagging efforts could optimize probability of capturing trans-Pacific movements by
510 targeting this area.

511 Isotopic analysis also provided information on foraging ecology of PBFT as large pelagic
512 predators in the eastern Pacific Ocean. Isotopic mixing model diet estimates for small PBFT
513 corroborate previous studies that show predominant feeding on 'forage prey' (e.g. sardine,
514 anchovy, pelagic red crab, small squids), with some feeding on macrozooplankton (e.g.

amphipods, euphausiids) (Pinkas 1971; Madigan et al. 2012b, 2015; Snodgrass et al. in prep). Access to larger PBFT allowed assessment of potential trophic level increase with PBFT size. PBFT $\delta^{15}N$ increased from ages 1 to 3, after which isotopic values and associated diet estimates were consistent (Figures 3 and 7 and Figure S2). High upwelling systems have been described as 'wasp-waist' systems in which one or few zooplanktivorous prey species, whose dominance fluctuates on yearly or decadal timescales (Chavez et al. 2003), support a large diversity and size range of predators (Cury et al. 2000; Bakun 2006). The single or several planktivorous species, which dominate this trophic link between plankton and large predators, constitutes the narrow 'wasp-waist' of such systems (Bakun 2006). PBFT from 3 to 6.3 years old fed predominantly on zooplanktivorous 'wasp-waist' prey (e.g. small forage fish, pelagic red crab; Figure 7). This contrasts with other eastern Pacific predators (e.g., California yellowtail *Seriola lalandi*, mako shark *Isurus oxyrinchus*) and western Pacific PBFT, which showed trophic upshifts with increasing size (Madigan et al. 2012b, 2016). The abundance of zooplanktivorous prey base may affect PBFT in the eastern Pacific, as has been proposed in the west (Polovina 1996). Large PBFT feeding on relatively small 'wasp-waist' prey is consistent with author observations of satiation feeding on pelagic red crabs and small anchovy in 2015-2016, and previous suggestions of feeding on red crab and forage fish spawning aggregations in regions of reduced upwelling (Boustany et al. 2010). Thus when highly abundant, pelagic red crab and other less energetically optimal prey can support a large biomass of PBFT, as do schooling fishes (Madigan et al. 2015). Consistent feeding by PBFT on small wasp-waist prey across size contrasts with trophic upshifts by larger PBFT in the west Pacific, an ecoregion of less overall productivity (Madigan et al. 2016).

Results here corroborate previous estimates of PBFT migration dynamics, provide quantitative estimates of migration patterns across age classes, and provide new information on the larger, potentially spawning-size PBFT in the eastern Pacific Ocean. Radiocesium became a less reliable tracer by 2013, but its utility in 2011 and 2012 facilitated the validation and application of a robust stable isotope tracer. The residency of larger PBFT in the eastern Pacific, and lack of recent migrants from the western Pacific after age 3, suggests that mortality of young age classes, and potentially availability of prey, dictate the abundance of older PBFT in the eastern Pacific and transitively the eventual contribution of this group to PBFT spawning stock. Collaborative and complementary bilateral research efforts across the Pacific will further elucidate trans-Pacific dynamics, and long-term studies are necessary to understand inter-annual variability of these dynamics. Ultimately, linking migration and residency patterns to environmental conditions such as ENSO and PDO will help to identify the underlying forcing mechanisms that influence the timing and frequency of trans-Pacific migrations. Such information can inform spatially structured stock assessments, the design of tagging or close-kin genetics studies that assume random sampling, and the design of recovery plan(s). Chemical tracers, particularly in combination with other collaborative PBFT research efforts, can be key elements in forthcoming strategies for improved management of PBFT.

ACKNOWLEDGMENTS

S. Zegers, J. Tallmon, J. Ewald, N. Wallsgrove, B. Popp, and C. Lyons for assistance in sample preparation and analysis. K. Franke from the Sportfishing Association of California was a liason with the sportfishing community in San Diego, CA. Captain M. Medak and the crew of the commercial passenger fishing vessel the *New Lo-An*, Captain P. Dupuy and the crew of the F/V

Ventura II, Sean, Rosie, Raymond, and employees at Fisherman's Processing, and all the recreational fishing anglers provided PBFT tissue samples. Numerous student volunteers and associated staff from NOAA's Southwest Fisheries Science Center in La Jolla, CA, USA assisted with sampling and processing. The detailed comments of two anonymous reviewers improved the manuscript. This material is partially based upon work supported by the National Science Foundation Postdoctoral Research Fellowship in Biology under Grant No. 1305791 and the John and Elaine French Environmental Fellowship (Harvard University Center for the Environment) to DJM. This research was supported in part by Grant No. 3423 from the Gordon and Betty Moore Foundation and No. 269672 from the European Commission to NF, and by the NOAA National Cooperative Research Program.

REFERENCES

Aires-da-Silva, A., Maunder, M., Deriso, R., Piner, K., and Lee, H. 2009. A sensitivity analysis of alternative natural mortality assumptions in the PBF stock assessment., International Scientific Committee for tuna and tuna-like species in the North Pacific Ocean (ISC).

Bakun, A. 2006. Wasp-waist populations and marine ecosystem dynamics: Navigating the "predator pit" topographies. Prog. Oceanogr. **68**: 271-288.

Baumann, H., Wells, R.J.D., Rooker, J.R., Zhang, S., Baumann, Z., Madigan, D.J., Dewar, H., Snodgrass, O.E., and Fisher, N.S. 2015. Combining otolith microstructure and trace elemental analyses to infer the arrival of juvenile Pacific bluefin tuna in the California current ecosystem. ICES J. Mar. Sci. **72**: 2128-2138.

581 Bayliff, W.H. 1993. Growth and age composition of northern bluefin tuna, *Thunnus thynnus*,
582 caught in the eastern Pacific Ocean, as estimated from length-frequency data, with
583 comments on Trans-Pacific migrations. Inter-Am. Trop. Tuna Comm. Bull.: 501-540.
584 Bayliff, W.H. 1994. A review of the biology and fisheries for northern bluefin tuna, *Thunnus*
585 *thynnus*, in the Pacific Ocean. FAO Fish. Tech. Pap. **336**: 244-295.
586 Bayliff, W.H., Ishizuka, Y., and Deriso, R. 1991. Growth, movement, and attrition of northern
587 bluefin tuna, *Thunnus thynnus*, in the Pacific Ocean, as determined by tagging. Inter-Am.
588 Trop. Tuna Comm. Bull. **20**: 3-94.
589 Block, B.A., Dewar, H., Blackwell, S.B., Williams, T.D., Prince, E.D., Farwell, C.J., Boustany,
590 A., Teo, S.L.H., Seitz, A., Walli, A., and Fudge, D. 2001. Migratory movements, depth
591 preferences, and thermal biology of Atlantic bluefin tuna. Science **293**: 1310-1314.
592 Block, B.A., Jonsen, I.D., Jorgensen, S.J., Winship, A.J., Shaffer, S.A., Bograd, S.J., Hazen,
593 E.L., Foley, D.G., Breed, G.A., Harrison, A.L., Ganong, J.E., Swithenbank, A., Castleton,
594 M., Dewar, H., Mate, B.R., Shillinger, G.L., Schaefer, K.M., Benson, S.R., Weise, M.J.,
595 Henry, R.W., and Costa, D.P. 2011. Tracking apex marine predator movements in a
596 dynamic ocean. Nature **475**: 86-90.
597 Boustany, A.M., Matteson, R., Castleton, M., Farwell, C., and Block, B.A. 2010. Movements of
598 Pacific bluefin tuna (*Thunnus orientalis*) in the Eastern North Pacific revealed with
599 archival tags. Prog. Oceanogr. **86**: 94-104.
600 Bradley, C.J., Madigan, D.J., Block, B.A., and Popp, B.N. 2014. Amino acid isotope
601 incorporation and enrichment factors in Pacific bluefin tuna, *Thunnus orientalis*. PLoS
602 ONE **9**: e85818.

603 Buchheister, A., and Latour, R.J. 2010. Turnover and fractionation of carbon and nitrogen stable
604 isotopes in tissues of a migratory coastal predator, summer flounder (*Paralichthys*
605 *dentatus*). Can. J. Fish. Aquat. Sci. **67**: 445-461.
606 Buesseler, K.O., Aoyama, M., and Fukasawa, M. 2011. Impacts of the Fukushima nuclear power
607 plants on marine radioactivity. Environ. Sci. Technol. **45**: 9931-9935.
608 Buesseler, K.O., Jayne, S.R., Fisher, N.S., Rypina, I.I., Baumann, H., Baumann, Z., Breier, C.F.,
609 Douglass, E.M., George, J., Macdonald, A.M., Miyamoto, H., Nishikawa, J., Pike, S.M.,
610 and Yoshida, S. 2012. Fukushima-derived radionuclides in the ocean and biota off Japan.
611 Proc. Natl. Acad. Sci. U.S.A. **109**: 5984-5988.
612 Carlisle, A.B., Kim, S.L., Semmens, B.X., Madigan, D.J., Jorgensen, S.J., Perle, C.R., Anderson,
613 S.D., Chapple, T.K., Kanive, P.E., and Block, B.A. 2012. Using stable isotope analysis to
614 understand migration and trophic ecology of northeastern Pacific white sharks
615 (*Carcharodon carcharias*). PLoS ONE **7**: e30492.
616 Chavez, F.P., Ryan, J., Lluch-Cota, S.E., and Ñiquen C, M. 2003. From anchovies to sardines
617 and back: multidecadal change in the Pacific Ocean. Science **299**: 217-221.
618 Chen, K.-S., Crone, P., and Hsu, C.-C. 2006. Reproductive biology of female Pacific bluefin
619 tuna *Thunnus orientalis* from south-western North Pacific Ocean. Fish. Sci. **72**: 985-994.
620 Clementz, M., and Koch, P. 2001. Differentiating aquatic mammal habitat and foraging ecology
621 with stable isotopes in tooth enamel. Oecologia **129**: 461-472.
622 Collette, B.B., Carpenter, K.E., Polidoro, B.A., Juan-Jordá, M.J., Boustany, A., Die, D.J., Elfes,
623 C., Fox, W., Graves, J., Harrison, L.R., McManus, R., Minte-Vera, C.V., Nelson, R.,
624 Restrepo, V., Schratwieser, J., Sun, C.L., Amorim, A., Brick Peres, M., Canales, C.,
625 Cardenas, G., Chang, S.K., Chiang, W.C., de Oliveira Leite, N., Harwell, H., Lessa, R.,

626 Fredou, F.L., Oxenford, H.A., Serra, R., Shao, K.T., Sumaila, R., Wang, S.P., Watson,
627 R., and Yáñez, E. 2011. High value and long life - double jeopardy for tunas and
628 billfishes. Science **333**: 291-292.
629 Cury, P., Bakun, A., Crawford, R.J.M., Jarre, A., Quiñones, R.A., Shannon, L.J., and Verheye,
630 H.M. 2000. Small pelagics in upwelling systems: patterns of interaction and structural
631 changes in "wasp-waist" ecosystems. ICES J. Mar. Sci. **57**: 603-618.
632 Davenport, S.R.B., Nicholas J. 2002. A trophic study of a marine ecosystem off southeastern
633 Australia using stable isotopes of carbon and nitrogen. Can. J. Fish. Aquat. Sci. **59**: 514-
634 530.
635 Domeier, M.L., Kiefer, D., Nasby-Lucas, N., Wagschal, A., and O'Brien, F. 2005. Tracking
636 Pacific bluefin tuna (*Thunnus thynnus orientalis*) in the northeastern Pacific with an
637 automated algorithm that estimates latitude by matching sea-surface-temperature data
638 from satellites with temperature data from tags on fish. Fish. Bull. **103**: 292-306.
639 Fisher, N.S., Beaugelin-Seiller, K., Hinton, T.G., Baumann, Z., Madigan, D.J., and Garnier-
640 LaPlace, J. 2013. An evaluation of radiation doses and associated risk from the
641 Fukushima nuclear accident to marine biota and human consumers of seafood. Proc. Natl.
642 Acad. Sci. U.S.A. **110**: 10670-10675.
643 Foreman, T.J., and Ishizuka, Y. 1990. Giant bluefin tuna off southern California, with a new
644 California size record. Calif. Fish Game, Fish Bull. **76**: 181-186.
645 Fromentin, J.-M., and Powers, J.E. 2005. Atlantic bluefin tuna: population dynamics, ecology,
646 fisheries and management. Fish Fish. **6**: 281-306.

Fujioka, K., Masujima, M., Boustany, A.M., and Kitagawa, T. 2015. Horizontal Movements of Pacific Bluefin Tuna. Pages 101-122 *in* T. Kitagawa and S. Kimura, editors. Biology and Ecology of Bluefin Tuna. CRC Press, Boca Raton, FL.

Furukawa, S., Fujioka, K., Fukuda, H., Suzuki, N., Tei, Y., and Ohshimo, S. 2016. Archival tagging reveals swimming depth and ambient and peritoneal cavity temperature in age-0 Pacific bluefin tuna, *Thunnus orientalis*, off the southern coast of Japan. Env. Biol. Fish, **100**: 35-48.

Graham, B.S., Koch, P.L., Newsome, S.D., McMahon, K.W., and Aurioles, D. 2010. Using Isoscapes to Trace the Movements and Foraging Behavior of Top Predators in Oceanic Ecosystems. Pages 299-318 *in* J. B. West, G. J. Bowen, T. E. Dawson, and K. P. Tu, editors. Isoscapes. Springer, Netherlands.

Hartog, J.R., Hobday, A.J., Matear, R., and Feng, M. 2011. Habitat overlap between southern bluefin tuna and yellowfin tuna in the east coast longline fishery – implications for present and future spatial management. Deep-Sea Res. Part II **58**: 746-752.

Inagake, D., Yamada, H., Segawa, K., Okazaki, M., Nitta, A., and Itoh, T. 2001. Migration of young bluefin tuna, *Thunnus orientalis* Temminck et Schlegel, through archival tagging experiments and its relation with oceanographic conditions in the Western North Pacific. Bull. Natl. Res. Inst. Far Seas Fish. **38**: 53-81.

ISC. 2012. Pacific bluefin stock assessment. International Scientific Committee for Tuna and Tuna-like Species in the North Pacific Ocean, Shimizu, Shizuoka, Japan.

ISC. 2014. Pacific Bluefin Stock Assessment. International Scientific Committee for Tuna and Tuna-like Species in the North Pacific Ocean, La Jolla, CA, USA.

669 ISC. 2016. Pacific Bluefin Stock Assessment. International Scientific Committee for Tuna and
670 Tuna-like Species in the North Pacific Ocean, La Jolla, CA, USA.
671 Itoh, T., Tsuji, S., and Nitta, A. 2003a. Migration patterns of young Pacific bluefin tuna
672 (*Thunnus orientalis*) determined with archival tags. Fish. Bull. **101**: 514-535.
673 Itoh, T., Tsuji, S., and Nitta, A. 2003b. Swimming depth, ambient water temperature preference,
674 and feeding frequency of young Pacific bluefin tuna (*Thunnus orientalis*) determined
675 with archival tags. Fish. Bull. **101**: 535-544.
676 Juan-Jordá, M.J., Mosqueira, I., Cooper, A.B., Freire, J., and Dulvy, N.K. 2011. Global
677 population trajectories of tunas and their relatives. Proc. Natl. Acad. Sci. U.S.A. **108**:
678 20650-20655.
679 Kintisch, E. 2015. 'The Blob' invades Pacific, flummoxing climate experts. Science **348**: 17-18.
680 Kitagawa, T., Boustany, A.M., Farwell, C.J., Williams, T.D., Castleton, M.R., and Block, B.A.
681 2007. Horizontal and vertical movements of juvenile bluefin tuna (*Thunnus orientalis*) in
682 relation to seasons and oceanographic conditions in the eastern Pacific Ocean. Fish.
683 Oceanogr. **16**: 409-421.
684 Kitagawa, T., Kimura, S., Nakata, H., Yamada, H., Nitta, A., Sasai, Y., and Sasaki, H. 2009.
685 Immature Pacific bluefin tuna, *Thunnus orientalis*, utilizes cold waters in the Subarctic
686 Frontal Zone for trans-Pacific migration. Environ. Biol. Fish. **84**: 193-196.
687 Kitagawa, T., Nakata, H., Kimura, S., Itoh, T., Tsuji, S., and Nitta, A. 2000. Effect of ambient
688 temperature on the vertical distribution and movement of Pacific bluefin tuna *Thunnus*
689 *thynnus orientalis*. Mar. Ecol. Prog. Ser. **206**: 251-260.
690 Kitagawa, T., Nakata, H., Kimura, S., Sugimoto, T., and Yamada, H. 2002. Differences in
691 vertical distribution and movement of Pacific bluefin tuna (*Thunnus thynnus orientalis*)

692 among areas: the East China Sea, the Sea of Japan and the western North Pacific. Mar.
693 Freshw. Res. **53**: 245-252.
694 Kitagawa, Y., Nishikawa, Y., Kuboto, T., and Okiyama, M. 1995. Distribution of
695 ichthyoplankton in the Japan Sea during summer, 1984, with special reference to
696 scombroid fishes. Bull. Jpn Soc. Fish. Oceanogr. **59**: 107–114.
697 Klaassen, M., Piersma, T., Korthals, H., Dekinga, A., and Dietz, M.W. 2010. Single-point
698 isotope measurements in blood cells and plasma to estimate the time since diet switches.
699 Funct. Ecol. **24**: 796-804.
700 Klecka, W.R. 1980. Discriminant Analysis. Sage Publications, Inc., Newbury Park, CA.
701 Logan, J.M., Jardine, T.D., Miller, T.J., Bunn, S.E., Cunjak, R.A., and Lutcavage, M.E. 2008.
702 Lipid corrections in carbon and nitrogen stable isotope analyses: comparison of chemical
703 extraction and modelling methods. J. Anim. Ecol. **77**: 838-846.
704 Madigan, D.J. 2015. Understanding Bluefin Migration Using Intrinsic Tracers in Tissues. Pages
705 211-224 *in* T. Kitagawa and S. Kimura, editors. Biology and Ecology of Bluefin Tuna.
706 CRC Press, Boca Raton, FL.
707 Madigan, D.J., Baumann, Z., Carlisle, A.B., Hoen, D.K., Popp, B.N., Dewar, H., Snodgrass,
708 O.E., Block, B.A., and Fisher, N.S. 2014. Reconstructing trans-oceanic migration
709 patterns of Pacific bluefin tuna using a chemical tracer toolbox. Ecology **95**: 1674-1683.
710 Madigan, D.J., Baumann, Z., and Fisher, N.S. 2012a. Pacific bluefin tuna transport Fukushima-
711 derived radionuclides from Japan to California. Proc. Natl. Acad. Sci. U.S.A. **109**: 9483-
712 9486.

713 Madigan, D.J., Baumann, Z., Snodgrass, O.E., Ergül, H.A., Dewar, H., and Fisher, N.S. 2013.
714 Radiocesium in Pacific bluefin tuna *Thunnus orientalis* in 2012 validates new tracer
715 technique. Environ. Sci. Technol.: 2287-2294.
716 Madigan, D.J., Carlisle, A.B., Dewar, H., Snodgrass, O.E., Litvin, S.Y., Micheli, F., and Block,
717 B.A. 2012b. Stable isotope analysis challenges wasp-waist food web assumptions in an
718 upwelling pelagic food web. Sci. Rep. **2**: e654.
719 Madigan, D.J., Carlisle, A.B., Gardner, L.D., Jayasundara, N., Micheli, F., Schaefer, K.M.,
720 Fuller, D.W., and Block, B.A. 2015. Assessing niche width of endothermic fish from
721 genes to ecosystem. Proc. Natl. Acad. Sci. U.S.A. **112**: 8350-8355.
722 Madigan, D.J., Chiang, W.-C., Wallsgrove, N.J., Popp, B.N., Kitagawa, T., Choy, C.A.,
723 Tallmon, J., Ahmed, N., Fisher, N.S., and Sun, C.-L. 2016. Intrinsic tracers reveal recent
724 foraging ecology of giant Pacific bluefin tuna at their primary spawning grounds. Mar.
725 Ecol. Prog. Ser. **553**: 253-266.
726 Madigan, D.J., Litvin, S.Y., Popp, B.N., Carlisle, A.B., Farwell, C.J., and Block, B.A. 2012c.
727 Tissue turnover rates and isotopic trophic discrimination factors in the endothermic
728 teleost, Pacific bluefin tuna (*Thunnus orientalis*). PLoS ONE **7**: e49220.
729 MAFF. 2015. Results of the inspection on radioactivity materials in fisheries products. Japanese
730 Ministry of Agriculture, Forestry, and Fisheries, Tokyo.
731 Moore, J.W., and Semmens, B.X. 2008. Incorporating uncertainty and prior information into
732 stable isotope mixing models. Ecol. Lett. **11**: 470-480.
733 Nakano, M., and Povinec, P.P. 2012. Long-term simulations of the 137Cs dispersion from the
734 Fukushima accident in the world ocean. J. Environ. Radioact. **111**: 109-115.

735 Nishikawa, Y. 1985. Average distribution of larvae of oceanic species of scombroid fishes,
736 1956-1982. Far Seas Fish. Res. Lab. **12**: 99.
737 Okiyama, M. 1974. Occurrence of the postlarvae of bluefin tuna, *Thunnus thynnus*, in the Japan
738 Sea. Jpn Sea Reg. Fish Res. Lab. Bull. **25**: 89–97.
739 Okochi, Y., Abe, O., Tanaka, S., Ishihara, Y., and Shimizu, A. 2016. Reproductive biology of
740 female Pacific bluefin tuna, *Thunnus orientalis*, in the Sea of Japan. Fish. Res. **174**: 30-
741 39.
742 Phillips, D., and Eldridge, P. 2006. Estimating the timing of diet shifts using stable isotopes.
743 Oecologia **147**: 195-203.
744 Phillips, D.L., and Gregg, J.W. 2003. Source partitioning using stable isotopes: coping with too
745 many sources. Oecologia **136**: 261-269.
746 Pikitch, E.K., Santora, C., Babcock, E.A., Bakun, A., Bonfil, R., Conover, D.O., Dayton, P.,
747 Doukakis, P., Fluharty, D., Heneman, B., Houde, E.D., Link, J., Livingston, P.A.,
748 Mangel, M., McAllister, M.K., Pope, J., and Sainsbury, K.J. 2004. Ecosystem-Based
749 Fishery Management. Science **305**: 346-347.
750 Pinkas, L. 1971. Bluefin tuna food habits. Fish. Bull. Cal. Dept. Fish Game **152**: 47-63.
751 Polovina, J.J. 1996. Decadal variation in the trans-Pacific migration of northern bluefin tuna
752 (*Thunnus thynnus*) coherent with climate-induced change in prey abundance. Fish.
753 Oceanogr. **5**: 114-119.
754 Post, D.M., Pace, M.L., and Hairston, N.G. 2000. Ecosystem size determines food-chain length
755 in lakes. Nature **405**: 1047-1049.

Revill, A., Young, J., and Lansdell, M. 2009. Stable isotopic evidence for trophic groupings and bio-regionalization of predators and their prey in oceanic waters off eastern Australia. Mar. Biol. **156**: 1241-1253.

Rooker, J.R., Secor, D.H., Zdanowicz, V.S., and Itoh, T. 2001. Discrimination of northern bluefin tuna from nursery areas in the Pacific Ocean using otolith chemistry. Mar. Ecol. Prog. Ser. **218**: 275-282.

Rypina, I.I., Jayne, S.R., Yoshida, S., Macdonald, A.M., Douglass, E.M., and Buesseler, K.O. 2013. Short-term dispersal of Fukushima-derived radionuclides off Japan: modeling efforts and model-data intercomparison. Biogeosci: 4973-4990.

Shimose, T., Tanabe, T., Chen, K.-S., and Hsu, C.-C. 2009. Age determination and growth of Pacific bluefin tuna, *Thunnus orientalis*, off Japan and Taiwan. Fish. Res. **100**: 134-139.

Shimose, T., and Wells, R.D. 2015. Feeding Ecology of Bluefin Tunas. Page 78 *in* T. Kitagawa and S. Kimura, editors. Biology and Ecology of Bluefin Tuna. CRC Press, Boca Raton, FL.

Smith, P.J., Griggs, L., and Chow, S. 2001. DNA identification of Pacific bluefin tuna (*Thunnus orientalis*) in the New Zealand fishery. New Zeal. J. Mar. Fresh. Res. **35**: 843-850.

Snodgrass, O., Dewar, H., Wells, R.J.D., and Kohin, S. in prep. Foraging ecology of tunas in the Southern California Bight.

Tanaka, Y., Mohri, M., and Yamada, H. 2007. Distribution, growth and hatch date of juvenile Pacific bluefin tuna *Thunnus orientalis* in the coastal area of the Sea of Japan. Fish. Sci. **73**: 534-542.

777 Tawa, A., Ishihara, T., Uematsu, Y., Ono, T., and Ohshimo, S. 2017. Evidence of westward
778 transoceanic migration of Pacific bluefin tuna in the Sea of Japan based on stable isotope
779 analysis. Mar. Biol. **164**: 94.
780 Weidel, B.C., Carpenter, S.R., Kitchell, J.F., and Vander Zanden, M.J. 2011. Rates and
781 components of carbon turnover in fish muscle: insights from bioenergetics models and a
782 whole-lake ^{13}C addition. Can. J. Fish. Aquat. Sci. **68**: 387-399.
783 Wells, R.J.D., Kinney, M.J., Kohin, S., Dewar, H., Rooker, J.R., and Snodgrass, O.E. 2015.
784 Natural tracers reveal population structure of albacore (*Thunnus alalunga*) in the eastern
785 North Pacific. ICES J Mar Sci **72**: 2118-2127.
786 Whitlock, R.E., Hazen, E.L., Walli, A., Farwell, C., Bograd, S.J., Foley, D.G., Castleton, M., and
787 Block, B.A. 2015. Direct quantification of energy intake in an apex marine predator
788 suggests physiology drives seasonal migrations. Sci Adv **1**: e1400270.
789

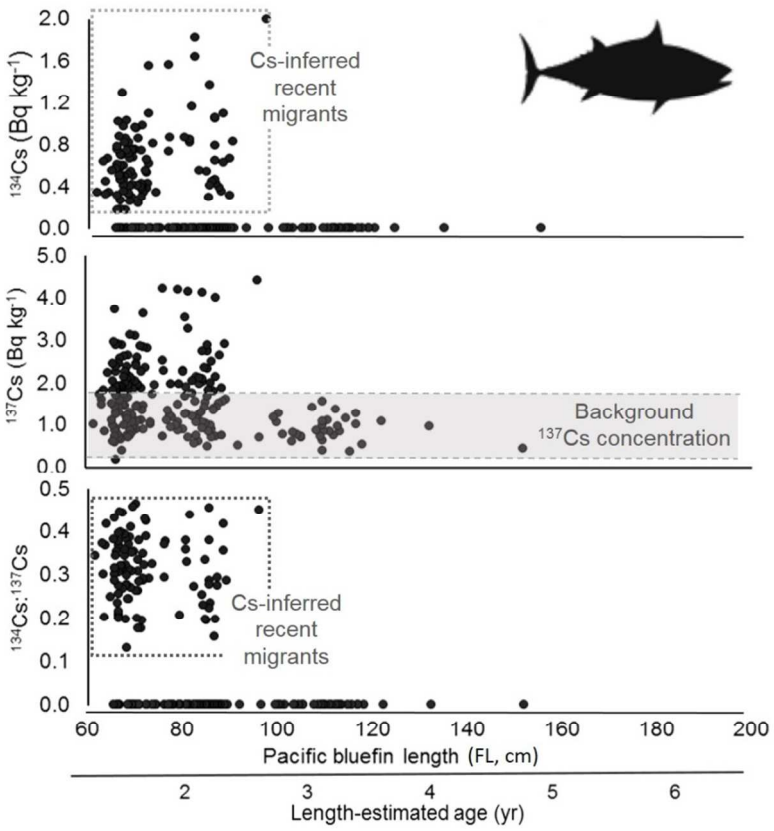

Figure 1. Radiocesium measurements in Pacific bluefin tuna (PBFT) sampled in 2012 and 2013. Each point (n = 272) represents measurements in an individual PBFT. Presence of ^{134}Cs and ^{134}Cs:^{137}Cs > 0 indicate recent migration from the western Pacific Ocean. Background levels of ^{137}Cs refer to ^{137}Cs distributed throughout the North Pacific Ocean in low levels resulting from nuclear weapons testing, primarily in the 1960s. Some of the smallest PBFT, known migrants from the western Pacific, had ^{134}Cs below detection, indicating that not all migrants accumulated measurable ^{134}Cs; all known migrants with undetectable ^{134}Cs were sampled in 2013. Analysis of ^{134,137}Cs was not performed on PBFT sampled in 2014 and 2015 due to its observed degradation as a tracer of trans-Pacific migration in 2013. Ages were estimated from length based on regression reported in Shimose et al. (2009).

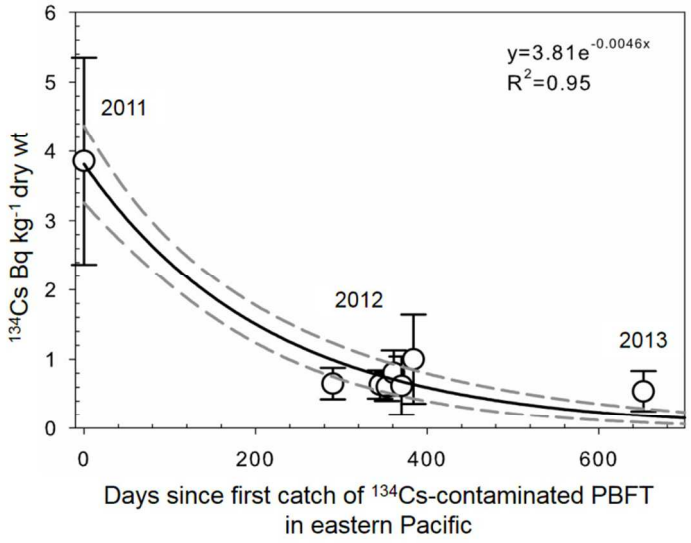

802

803

804 **Figure 2. Decline of ^{134}Cs in PBFT caught off California in summers of 2011, 2012 and**

805 **2013.** The rate at which ^{134}Cs declined in PBFT caught off California equals to 0.0046 ±0.0004

806 (±SE) d^{-1}, translating to effective half-life of ^{134}Cs in these PBFT of 151 days. This calculation

807 excludes one individual that was caught in the summer of 2012 with unusually high ^{134}Cs

808 activity (7.4 ±0.6 Bq kg^{-1} dry wt.), which was treated as an outlier.

809

810

811

812

813

814

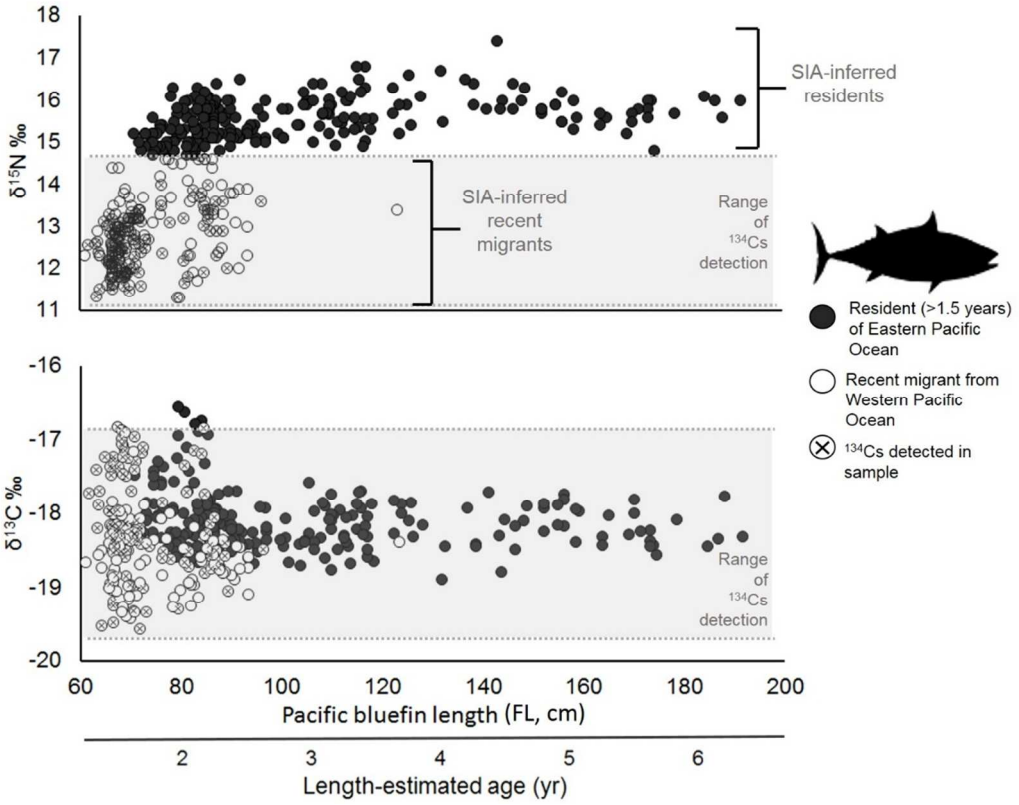

Figure 3. Stable isotope ratios of $\delta^{15}N$ and $\delta^{13}C$ across sampled sizes of Pacific bluefin tuna (PBFT) from 2012 to 2015. Each point represents measurements in an individual PBFT. When coupled with ^{134}Cs analyses, there were clear differences between resident and migrant $\delta^{15}N$ values. $\delta^{13}C$ values of residents and migrants showed high overlap, demonstrating that $\delta^{15}N$ but not $\delta^{13}C$ can be used effectively to ascertain recent migration patterns of PBFT in the eastern Pacific Ocean. Ages were estimated from length based on regression reported in Shimose et al. (2009).

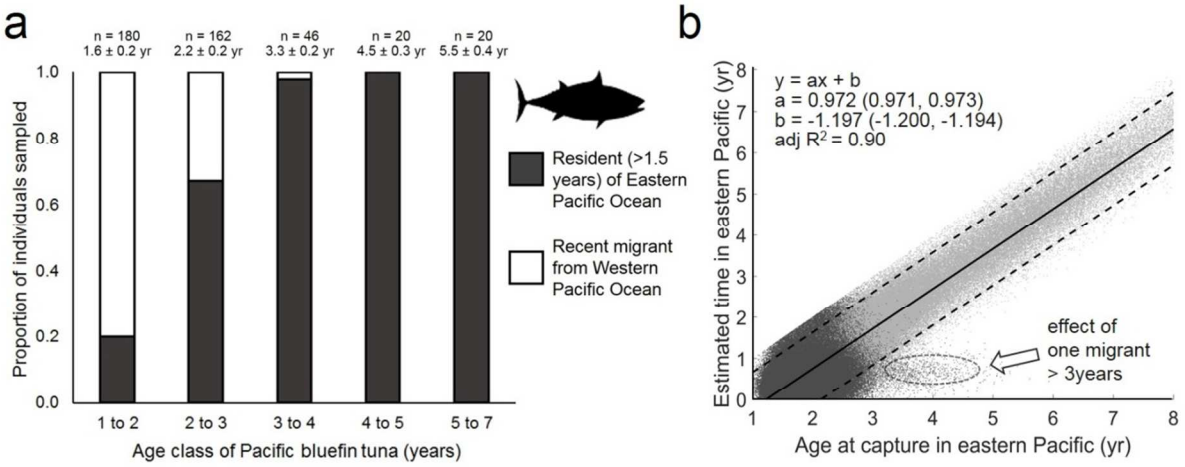

Figure 4. Migration dynamics of 428 age 1-7 Pacific bluefin tuna (PBFT) sampled from 2012 to 2015. (a) Proportion of residents to migrants by age class and (b) estimated residency time in the eastern Pacific Ocean by fish age for PBFT captured off southern California, USA. Residents and migrants were categorized by radiocesium and stable isotope analysis. In (a), sample size and mean age (± SD) shown above bar for each age class. All residents in age class 1-2 were 1.6 to 2.0 years old; see Figure S1 for a breakdown of age class 1-2. (b) Estimated residency time for each PBFT from bootstrap analysis (light gray points: residents, dark gray points: migrants), overall residency time (solid line) and 95% confidence interval (stippled lines) based on linear fit to bootstrap estimates.

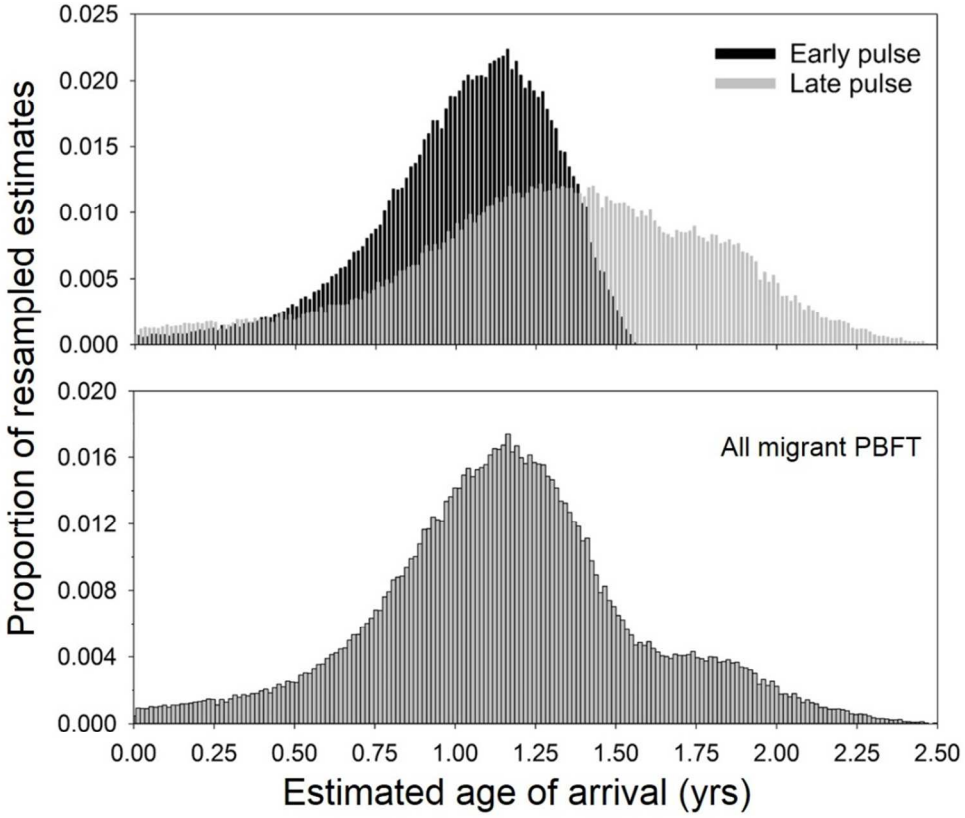

844

845

846 **Figure 5. Estimated ages of arrival of Pacific bluefin tuna (PBFT) in the eastern Pacific**
847 **Ocean from 2011 to 2015.** Arrival dates based on isotopic clock technique using $\delta^{15}N$ values of
848 PBFT (×1000 iterations or estimates individual^{-1}). PBFT were sampled between 2012 and 2015,
849 and ages estimated from length from regression reported in Shimose et al. (2009). 'Early pulse'
850 and 'Late pulse' in top panel refers to small (60-80 cm) and larger (80-100 cm) PBFT,
851 respectively, characterized as recent migrants to the eastern Pacific Ocean. Bottom panel shows
852 arrival times for all migrant PBFT, with a major pulse of migrant PBFT between age 1 and 1.3
853 yrs and a second smaller pulse at age 1.5 to 2 yrs. Note a small proportion of arrival age <0.5;
854 this does not suggest newly hatched PBFT in the eastern Pacific, but is an artefact of
855 bootstrapping estimates of multiple parameter outliers.

856

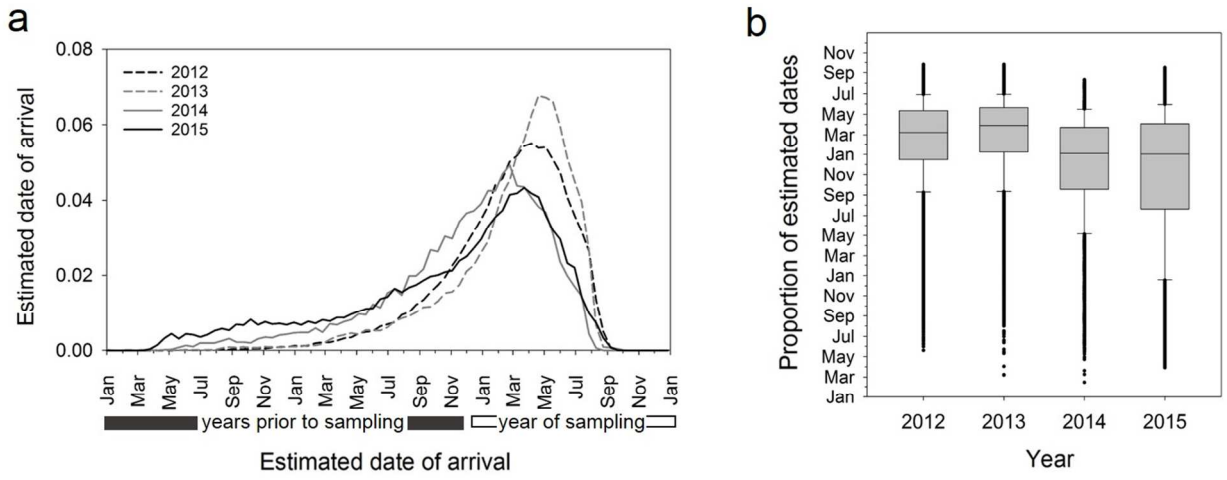

857
858
859 **Figure 6. Estimated arrival times of Pacific bluefin tuna in the eastern Pacific Ocean for**
860 **years 2012-2015.** Arrival dates based on bootstrapped isotopic clock technique using $\delta^{15}N$
861 values of PBFT (×1000 iterations or estimates individual^{-1}). (a) Histograms showing estimated
862 arrival times of PBFT by year sampled. (b) Tukey boxplots of estimated arrival dates used to
863 generate histograms in (a). Box shows median and interquartile range (IQR) and solid points
864 show outliers. In 2014 and 2015, median arrival time was earlier and overall arrival times were
865 more broadly distributed. Outlier values are largely a product of bootstrapped estimates using
866 extreme values of multiple parameters of isotopic clock approach.
867
868
869
870
871
872
873

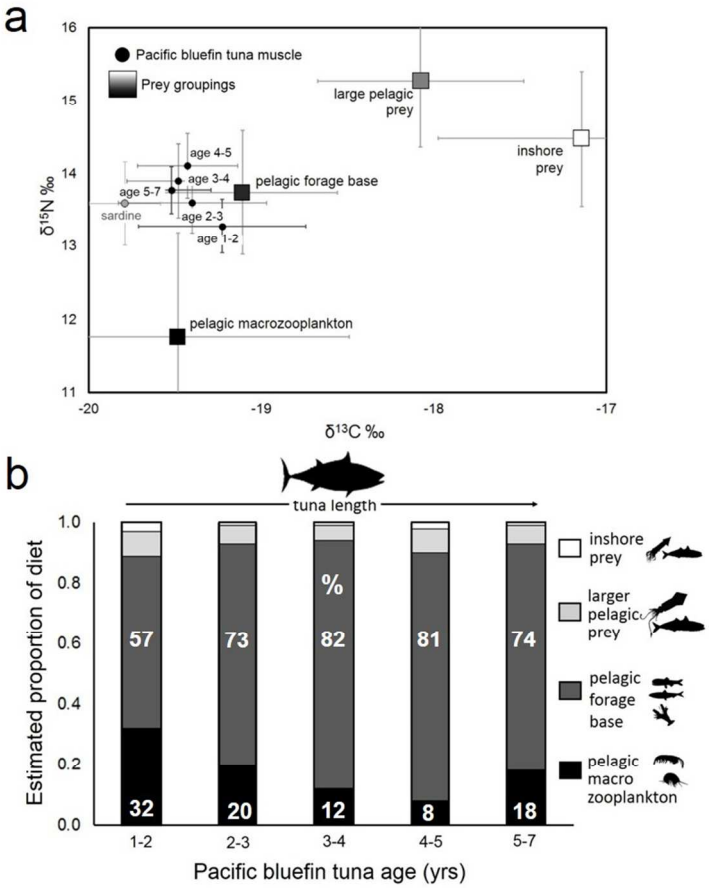

Figure 7. Isotopic reconstruction of resident Pacific bluefin tuna (PBFT) diet in the eastern Pacific Ocean. (a) Biplot of $\delta^{13}C$ and $\delta^{15}N$ values (mean ± SD) for PBFT grouped by age class (small black circles) and prey groups (large squares) in the eastern Pacific Ocean. Pelagic macrozooplankton includes krill and amphipods; pelagic forage base represents a diverse group of zooplanktivorous fish and small cephalopods. PBFT values are grouped by age class as indicated. (b) Stable isotope-based estimates of proportional input of four prey groups into diet of PBFT in the eastern Pacific Ocean. Estimates are from Bayesian mixing model (MixSIR) and based on $\delta^{15}N$ and $\delta^{13}C$ values of PBFT and prey muscle tissue. Estimated percentage of diet shown for the two major diet inputs.

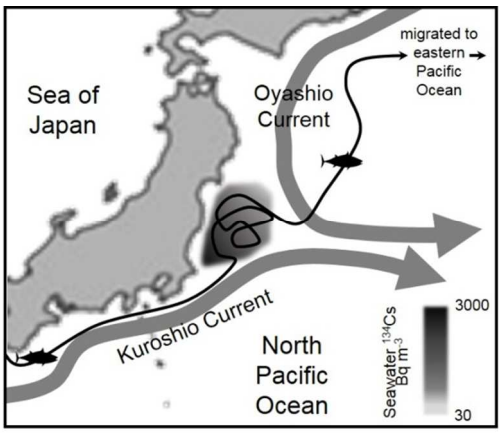

Figure 8. Migration route of an electronically tagged juvenile Pacific bluefin tuna (PBFT) coincides with regions of high Fukushima-derived radiocesium. Major currents, seawater radiocesium levels, and the simplified migration route of one PBFT off Japan (Kitagawa et al. 2009). High seawater levels of ^{134}Cs in June 2011 (shaded polygon) were constrained to the Kuroshio-Oyashio transition region, with the Kuroshio Current acting as a southern boundary (Rypina et al. 2013). One electronically tagged PBFT showed residency in this region before migration to the eastern Pacific Ocean (black arrow) (Kitagawa et al. 2009). The high detection rate of ^{134}Cs in PBFT in the eastern Pacific suggests this region as a migratory precursor to trans-Pacific migration. Simplified migration route and seawater levels modified from Kitagawa et al. (2009) and Rypina at al. (2013), respectively.